Physica B 439 (2014) 189–192

Contents lists available at ScienceDirect

Physica B

journal homepage: www.elsevier.com/locate/physb

Synthesis, optical and morphological characterization of doped InP/ZnSe NCs

Paul Mushonga [a], Immaculate L.A. Ouma [a], Abram M. Madiehe [b], Mervin Meyer [b], Francis B. Dejene [c], Martin O. Onani [a,*]

[a] Department of Chemistry, University of the Western Cape, Private Bag X17, Bellville 7535, South Africa
[b] Department of Biotechnology, University of the Western Cape, Private Bag X17, Bellville 7535, South Africa
[c] Department of Physics, University of the Free State (QwaQwa Campus), Private Bag X13, Phuthaditjhaba 9866, South Africa

ARTICLE INFO

Available online 12 December 2013

Keywords:
Nanocrystals
Growth-doping
InP/ZnSe
Ag-dopant
Co-dopant
Fe-dopant

ABSTRACT

We report on the Ag-, Fe-, and Co-doping of InP/ZnSe QDs using the growth-doping method. Doping the InP/ZnSe NCs with Ag caused a red-shift in the emission spectra with increasing dopant levels while the PL intensity decreased. Fe-doping resulted in blue-shifted emission spectra. The cobalt-doping (Co-doping) had no effect on the emission peak position. Instead, it had a quenching effect on the PL intensities. The HRTEM images showed well-defined lattice fringes for the doped InP/ZnSe NCs while the XRD analyses showed that they retained their zinc blende structure even after doping.

1. Introduction

Colloidal semiconductor nanocrystals (NCs) or quantum dots (QDs) are nanometer-sized clusters that are composed of a few hundreds to several thousands of atoms from groups II–VI, III–V or IV–VI [1,2]. These semiconductor NCs have unique size-tuneable optical and electronic properties. The intentional and controlled introduction of impurities into these nanomaterials tunes their optoelectronic, mechanical and magnetic properties [3–5]. The dopants create local quantum states that lie within the bandgaps [6]. These quantum states alter the band structures of the doped NCs and hence their optical properties. Relaxation via these impurity states (rather than surface states) improves the radiative efficiency for localized impurity-induced transition [7]. The three reported methods for the doping of nanocrystals involve the nucleation, growth-doping [8] and isocrystalline core/shell [9]. This paper reports on the one-pot synthesis of luminescent doped-InP/ZnSe NCs using Ag, Fe and Co as dopants. The growth-doping method was used where both core-doping and subsequent shell growth occurred in one reactor.

2. Experimental

All reagents used in this study were of analytical grade and were used as received. Indium acetate ($In(OAc)_3$), palmitic acid, zinc undecylenate, silver nitrate, selenium powder, trioctylphosphine (TOP), 1-octadecene (ODE, 90%), tetramethylammonium hydroxide pentahydrate, tris(trimethylsilyl)phosphine ($P(TMS)_3$, 95%), methanol, acetone, 2-propanol, hexane and chloroform were supplied by Sigma Aldrich. Sodium hydroxide, cobalt(II) chloride hexahydrate and iron(II) chloride tetrahydrate were purchased from Saarchem.

2.1. Synthesis

2.1.1. Preparation of precursors

2.1.1.1. Preparation of selenium and Zn injection solutions. The procedures for the preparation of selenium [10] and zinc injection solutions [11] were adapted from literature with some modifications – zinc undecylenate was used instead of zinc stearate and TOP was added to the reaction system. The selenium injection solution (TOPSe) (0.1 M) was prepared by dissolving selenium powder in a mixture of ODE (9 mL) and TOP (1 mL) at 140 °C affording a clear solution. The zinc injection solution (0.1 M) was prepared by dissolving zinc undecylenate (0.432 g, 0.001 mol) in a mixture of ODE (9 mL) and TOP (1 mL) at 140 °C.

2.1.1.2. Preparation of silver palmitate. A procedure by Uznanski and Bryszewska [12] was adopted for the synthesis of silver palmitate. Palmitic acid (5.12 g, 0.02 mol) and deionized water (200 mL) were added to a two-necked flask and heated at 80 °C with stirring. NaOH (0.72 g, 0.018 mol) in water (4 mL) was then added giving a clear solution. $AgNO_3$ (3.058 g, 0.018 mol) in water

* Corresponding author. Tel.: +27 21 959 3050; fax: +27 21 959 1400.
E-mail address: monani@uwc.ac.za (M.O. Onani).

0921-4526/$ - see front matter © 2013 Elsevier B.V. All rights reserved.
http://dx.doi.org/10.1016/j.physb.2013.12.009

(25 mL) was added precipitating silver palmitate as a white product. The product was dried at 60 °C overnight in air.

2.1.1.3. Preparation of cobalt(II) palmitate. Cobalt(II) palmitate was synthesized following a procedure by Acharya and Pradhan with some modifications [13]. Palmitic acid (5.128 g, 0.02 mol), was added to methanol (20 mL) in a two-necked round bottomed flask and heated to 60 °C to obtain a clear solution. Tetramethylammonium hydroxide pentahydrate (TMAH) (3.625 g, 0.02 mol) was dissolved separately in methanol (10 mL) and transferred into a dropping funnel. The TMAH solution was then added drop wise to the palmitic acid solution with stirring over 20 min to complete the reaction. Separately, $CoCl_2 \cdot 6H_2O$ (2.379 g, 0.01 mol) was dissolved in methanol (10 mL) and again added drop wise to the above solution with vigorous stirring. A faint pink product, cobalt(II) palmitate was obtained. The product was filtered, washed with methanol and dried under vacuum.

2.1.1.4. Preparation of iron(II) palmitate. Iron(II) palmitate was synthesized following the same procedure as for silver palmitate. Iron(II) chloride tetrahydrate (4.012 g, 0.02 mol) was dissolved in methanol (100 mL). Palmitic acid (10.313 g, 0.04 mol) and methanol (100 mL) were added to a two-necked flask, heated at 80 °C with stirring and slowly added to the above solution. NaOH (0.815 g, 0.02 mol) in water (20 mL) was added precipitating brown iron(II) palmitate. The product was filtered, washed with methanol and dried under vacuum.

2.1.2. Synthesis of M:InP/ZnSe (M=Ag, Co, and Fe)

All experiments involving the doping of InP/ZnSe nanocrystals with transition metal elements (Ag, Fe and Co) were carried out following a literature procedure, with some modifications [14]. The Ag-doped InP/ZnSe NCs were synthesized at a doping level of 5% Ag with respect to P. In the synthesis, indium acetate (0.2 mmol) was mixed with palmitic acid (0.8 mmol) and ODE (4 mL) in a three-necked flask in the glove box. The flask was sealed and transferred to a Schlenk line and heated to 120 °C and kept under vacuum for 1.5 h. The system was then purged with argon and then heated to 300 °C. On reaching 300 °C, a freshly prepared injection solution of $P(TMS)_3$ in TOP (0.1 mmol in 0.5 mL TOP prepared in the glove box) was injected rapidly under argon flow. For the growth of the InP core, the reaction mixture was kept at around 270 °C for 1 h. The temperature was lowered to 130 °C and silver palmitate (0.5 mL, 0.01 M) was added. The temperature was raised to 210 °C for 1 h to effect the doping. The temperature was then lowered to 150 °C for the addition of zinc and selenium precursors for the ZnSe shell. Zinc undecylenate (0.6 mL, 0.1 M) and TOPSe (0.6 mL, 0.1 M) were added with a 10 min interval between the two injections. The temperature was raised to 230 °C for 1 h. The temperature was again lowered to 150 °C and zinc undecylenate (0.8 mL, 0.1 M) and TOPSe (0.8 mL, 0.1 M) were added with a 10 min interval between the injections. The temperature was raised to 230 °C for 1 h. The Ag dopant levels were varied 0%, 5% and 10% with respect to moles of phosphorus. Co: InP/ZnSe and Fe:InP/ZnSe NCs were synthesized in a similar manner with doping levels of 0%, 15% and 20% Co as well as 0%, 5% and 10% Fe using cobalt(II) palmitate and iron(II) palmitate as dopant sources respectively.

2.2. Characterization

Photoluminescence (PL) spectra were recorded on a HORIBA Nanolog FL3-22-TRIAX. Samples for PL analysis were dispersed in hexane. The values of PL intensity were normalized simply by dividing the PL intensity by the highest PL intensity value corresponding to the emission peak. TEM studies were performed on a TECNAI F30ST TEM. The samples for TEM studies were prepared by placing a hexane solution of the nanocrystals on ultrathin carbon-film-coated copper grids. XRD analysis was carried out at iThemba Labs, Cape Town using a Bruker AXS D8 Advanced Diffractometer equipped with a CuKα (λ=1.5418 Å) X-ray source.

3. Results and discussion

3.1. Optical characterization

Luminescent transition metal doped InP/ZnSe NCs were successfully synthesized using a growth-doping method. Fig. 1(a)–(c) shows the normalized PL spectra of Ag, Co and Fe-doped InP/ZnSe NCs. The introduction of Ag dopant caused a red-shift in the emission spectra of the InP/ZnSe NCs. The emission peak positions were 592, 598 and 613 nm for Ag-dopant levels of 0%, 5% and 10%, respectively. A similar red-shift was also reported by Banin and co-workers when they prepared Ag-doped InAs NCs [15]. They reported that Ag^+ ions act as substitutional impurities (as opposed to interstitial impurities) in III–V semiconductors. This is due to their large ionic radii (129 pm) compared to In^{3+} ions (94 pm). The Ag^+ ions distort the crystal structure of the III–V systems leading to band-tailing and consequently to the red-shift in the emission spectrum. A pronounced decrease in PL intensity with increasing Ag dopant levels was realized. Georgekutty et al. reported a similar observation where Ag-dopant induced the quenching of PL intensity in the ZnO nanoparticles. This phenomenon was attributed to a decrease in electron–hole recombination [16]. Further, doping with cobalt gave no change in the emission spectrum. However, a decrease in PL intensity with increasing Co-doping level from 15% to 20% was observed. A similar observation was made by Vatankhah et al. [17]. They reported that the quenching point for Co:ZnS nanocrystals was 0.1% of the dopant. An increase in the level of cobalt impurity to 5% resulted in continuous decrease in the fluorescence signal. In another report of Co:CdS NCs, the emission intensity decrease for a 6% dopant level was attributed to an even dopant incorporation in the CdS nanocrystals [18]. Peng et al. equally reported the suppression of exciton emission with increasing Co dopant levels in a ZnO system [19]. This was because of an increase in the distortion of host lattice and defects as more dopant ions displaced host cations. The PL spectra of Fe-doped InP/ZnSe NCs (Fig. 1(c)) exhibited a blue-shift with increase in dopant level from 1% to 5%. The emission peaks were 592 and 566 nm for the Fe dopant levels of 1% and 5% respectively. A similar blue-shift was observed by Yang et al. when they fabricated Fe:ZnSe NCs [20]. However, the blue-shift was reported to be due to a decrease in the reaction rate with the incorporation of the dopant ions. This was confirmed by nanoparticle size reduction and bandgap increase. A decrease in emission intensity was also observed with an increase in dopant level from 1% to 5% indicating that the iron dopant acted to quench the fluorescence from the InP core. The quenching effect of iron in Fe-doped ZnS was ascribed to the trapping of electrons by Fe centers culminating in non-radiative recombination of excitons [21].

3.2. Structural characterization

3.2.1. TEM studies

Fig. 2(a)–(c) shows the TEM micrographs of the Ag, Co and Fe-doped InP/ZnSe NCs. The micrographs exhibit lattice fringes indicating the good crystallinity of the nanocrystals. The particle sizes as determined by TEM were 3.73, 4.49 and 4.23 nm for Ag (5%), Co (15%) and Fe (5%) doped InP/ZnSe NCs respectively. The EDX analysis showed the presence of dopant ions.

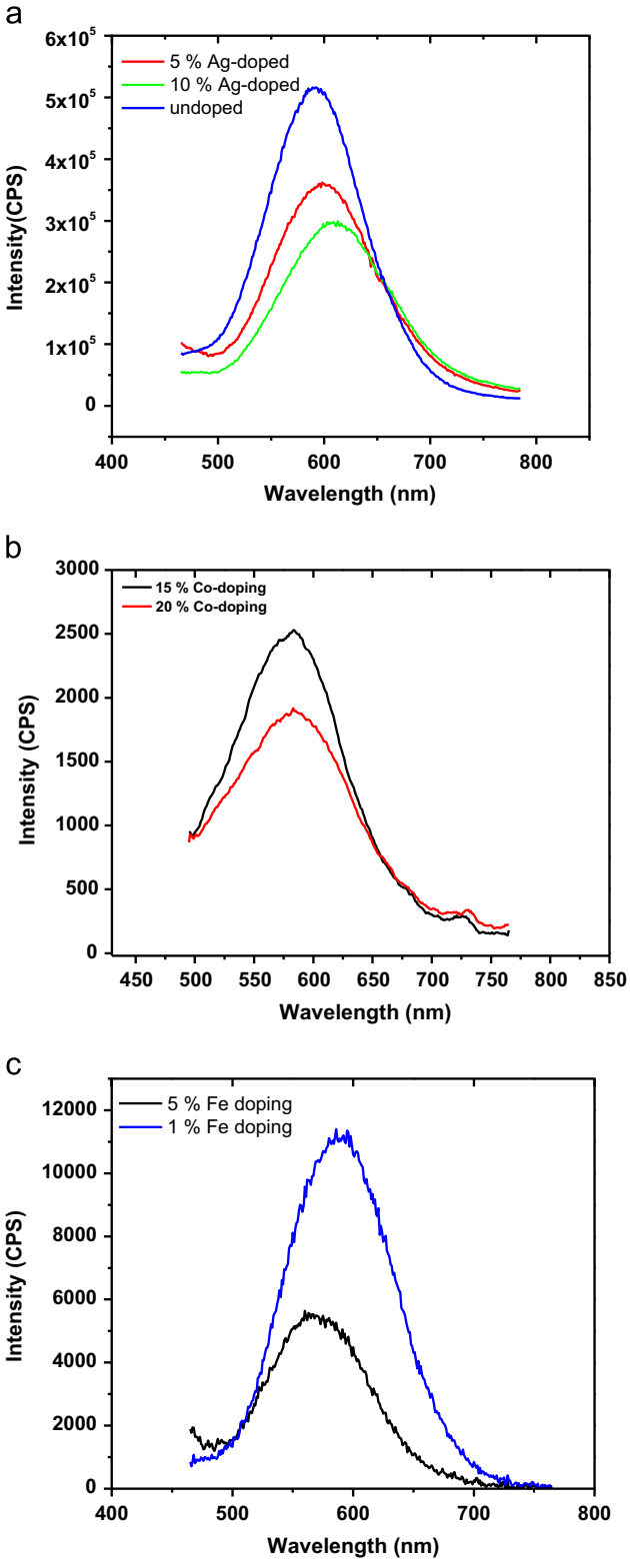

Fig. 1. Normalized PL spectra of (a) Ag-, (b) Co- and (c) Fe-doped InP/ZnSe NCs.

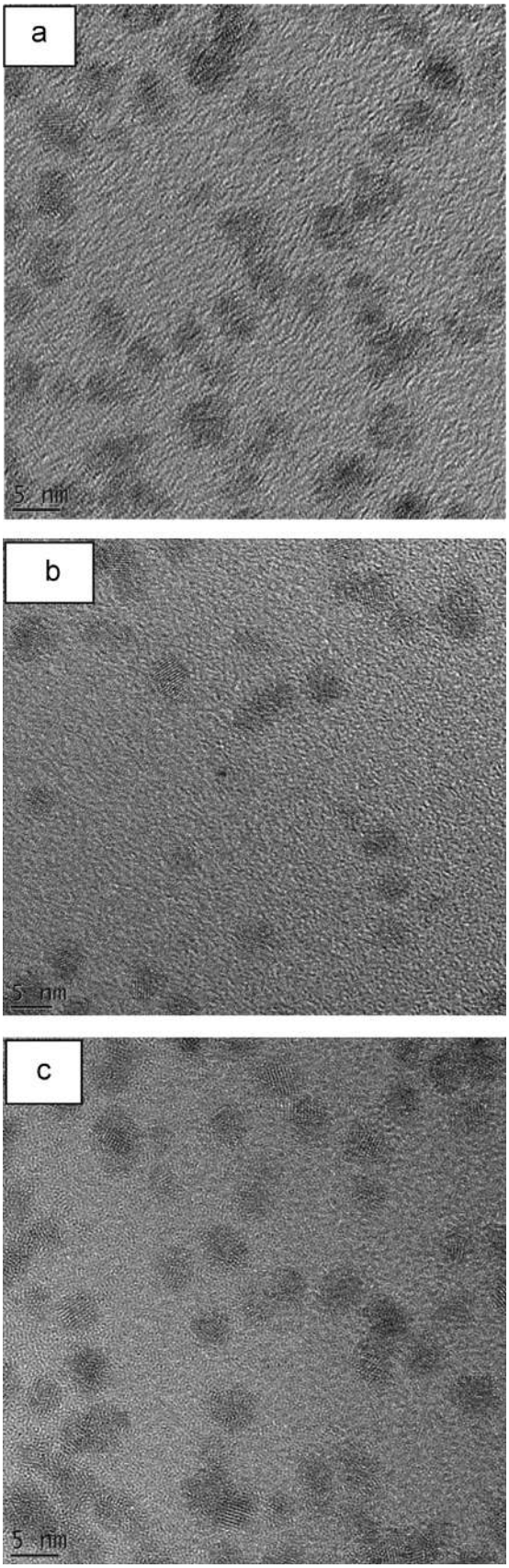

Fig. 2. TEM micrographs of (a) 5% Ag, (b) 15% Co and (c) 10% Fe-doped InP/ZnSe NCs.

3.2.2. *XRD studies*

Fig. 3 shows the XRD pattern for the Ag-doped InP/ZnSe NCs. From the XRD diffractogram, three broad peaks with 2θ values of 26.28°, 43.61° and 51.62° corresponding to (1 1 1), (2 2 0) and (3 1 1) reflecting planes respectively proved that the Ag-doped InP/ZnSe NCs had a cubic zinc blende structure similar to pure InP/ZnSe. Manganese-doped InP nanocrystals have also retained the cubic zinc blend structure [22]. No shifts in the 2θ angles were observed in the XRD pattern for the Ag-doped InP/ZnSe nanocrystals. Incorporation of Ag dopant ions into a crystal lattice

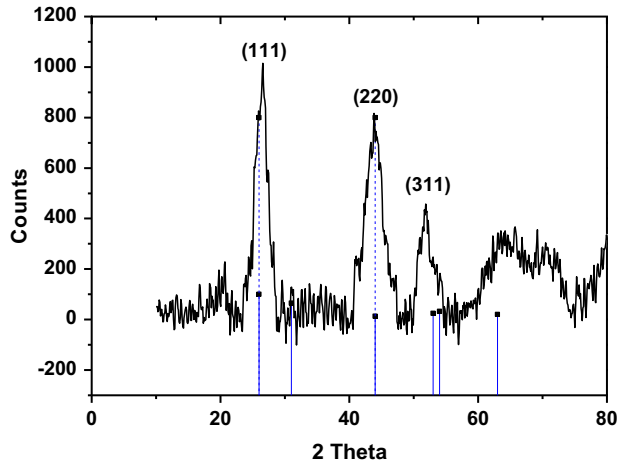

Fig. 3. XRD pattern for 5% Ag-doped InP/ZnSe nanocrystals.

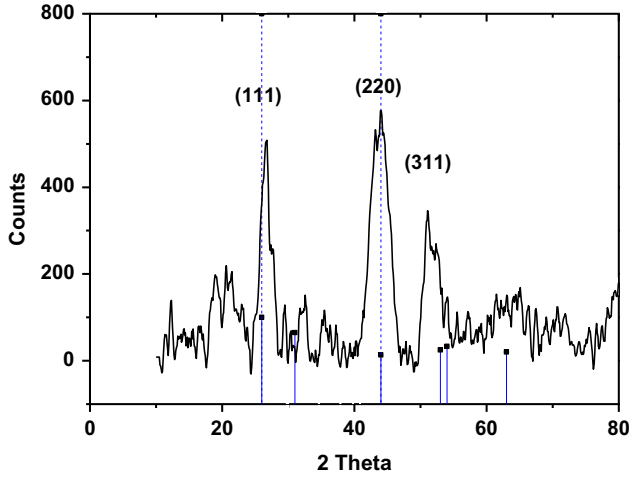

Fig. 4. XRD pattern for 15% Co-doped InP/ZnSe nanocrystals.

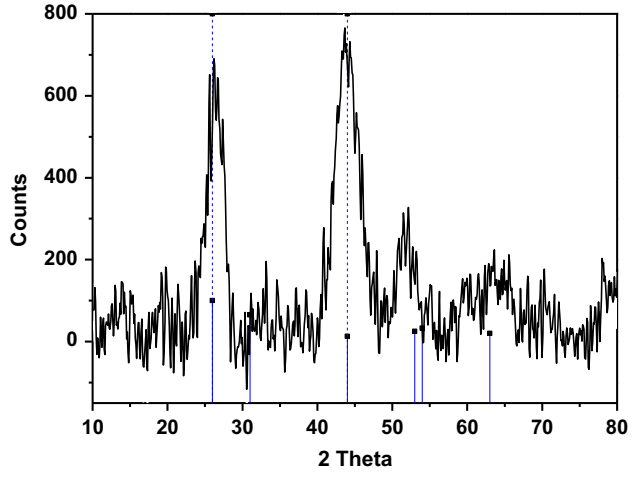

Fig. 5. XRD pattern for 1% Fe-doped InP/ZnSe nanocrystals.

(via substitution) has been reported to cause a corresponding shift in the 2θ angles [23]. Where such shifts are absent, as in the case of Ag:ZnO, this has been interpreted to signify segregation of dopant ions in the grain boundaries of nanocrystal lattice. There were no characteristic peaks for silver impurity phases such as peaks at 38.2°, 44.4°, 64.4° and 77.3° corresponding to (1 1 1), (2 0 0), (2 2 0) and (3 1 1) planes respectively [24].

Figs. 4 and 5 show the XRD diffractograms of Co- and Fe-doped InP/ZnSe NCs. Once again, the diffraction peaks indicated that the zinc blende crystal structure was retained after doping with both cobalt and iron. There were no cobalt nanocrystal impurity phases observed in Fig. 4 [25]. The group of Voyles reported Fe-doped ZnO where the XRD pattern for different concentrations of the dopant and aging times corresponded to the wurtzite structure of the pure ZnO nanocrystals [26].

4. Conclusions

Transition metal (Ag, Fe, and Co) doped InP/ZnSe nanocrystals were successfully synthesized following the growth doping method. In all the experiments, high quality nanocrystals were obtained as exhibited by their TEM micrographs. All the doped nanocrystals exhibited a photoluminescence quenching effect which was attributed to a decrease in the electron–hole recombination with increasing dopant levels.

Acknowledgments

The authors acknowledge DST/Mintek NIC and NRF for funding.

References

[1] P. Mushonga, M.O. Onani, A.M. Madiehe, M. Meyer, J. Nanomater. 2012 (2012) 869284.
[2] P. Mushonga, M.O. Onani, A.M. Madiehe, M. Meyer, Mater. Lett. 95 (2013) 37.
[3] S.C. Erwin, L. Zu, M.I. Haftel, A.L. Efros, T.A. Kennedy, D.J. Norris, Nature 436 (2005) 91.
[4] C.A. Stowell, R.J. Wiacek, A.E. Saunders, B.A. Korgel, Nano Lett. 3 (2003) 1441.
[5] P. Lommens, F. Loncke, P.F. Smet, F. Callens, D. Poelman, H. Vrielinck, Z. Hens, Chem. Mater. 19 (2007) 5576.
[6] D. Bera, L. Qian, T.-K. Tseng, P.H. Holloway, Materials 3 (2010) 2260.
[7] R.N. Bhargava, J. Lumin. 70 (1996) 85594.
[8] N. Pradhan, D. Goorskey, J. Thessing, X. Peng, J. Am. Chem. Soc. 127 (2005) 17586.
[9] P.V. Radovanovic, D.R. Gamelin, J. Am. Chem. Soc. 123 (2001) 12207.
[10] A. Narayanaswamy, L.F. Feiner, A. Meijerink, P.J. van der Zaag, ACS Nano 3 (2009) 2539.
[11] A. Narayanaswamy, L.F. Feiner, A. Meijerink, P.J. van der Zaag, ACS Nano 3 (2009) 2539.
[12] P. Uznanski, E. Bryszewska, J Mater. Sci. 45 (2010) 1547.
[13] S. Acharya, N. Pradhan, J. Phys. Chem. C 115 (2011) 19513.
[14] R. Xie, X. Peng, J. Am. Chem. Soc. 131 (2009) 10645.
[15] D. Mocatta, G. Cohen, J. Schattner, O. Millo, E. Rabani, U. Banin, Science 332 (2011) 77.
[16] R. Georgekutty, M.K. Seery, S.C. Pillai, J. Phys. Chem. C 112 (2008) 13563.
[17] C. Vatankhah, M.H. Yuosefi, A.A. Khosravi, M. Savarian, Eur. Phys. J. Appl. Phys. 48 (2009) 20601.
[18] L. Saravanan, A. Pandurangan, R. Jayavel, J. Nanopart. Res. 13 (2011) 1621.
[19] Y.Z. Peng, T. Liew, W.D. Song, C.W. An, K.L. Teo, T.C. Chong, J. Supercond. 18 (2005) 97.
[20] L. Yang, J. Zhu, D. Xiao, RSC Adv. 2 (2012) 8179.
[21] S. Selmani, H. Abdullah, S. Shaari, R. Abd-Shukor, Funct. Mater. Lett. 4 (2011) 101.
[22] Y. Sahoo, P. Poddar, H. Srikanth, D.W. Lucey, P.N. Prasad, J. Phys. Chem. B 109 (2005) 15221.
[23] R. Georgekutty, M.K. Seery, S.C. Pillai, J. Phys. Chem. C 112 (2008) 13563.
[24] M.A.M. Khan, S. Kumar, M. Ahamed, S.A. Alrokayan, M.S. AlSalhi, Nanoscale Res. Lett. 6 (2011) 434.
[25] Y. Bao, A.B. Pakhomov, K.M. Krishnan, J. Appl. Phys. 97 (2005) 10J317.
[26] A. Parra-Palomino, O. Perales-Perez, R. Singha, M. Tomar, J. Hwang, P.M. Voyles, J. Appl. Phys. 103 (2008) 07D121.